ResearchGate

See discussions, stats, and author profiles for this publication at: https://www.researchgate.net/publication/232764170

Stabilization of Colloidal Suspensions: Competing Effects of Nanoparticle Halos and Depletion Mechanism

ARTICLE *in* LANGMUIR · NOVEMBER 2012

Impact Factor: 4.46 · DOI: 10.1021/la303547m · Source: PubMed

CITATIONS
10

READS
51

4 AUTHORS, INCLUDING:

To Ngai
The Chinese University of Hong Kong
94 PUBLICATIONS **1,304** CITATIONS
SEE PROFILE

Guanqing Sun
The Chinese University of Hong Kong
15 PUBLICATIONS **127** CITATIONS
SEE PROFILE

Zifu Li
Georgia Institute of Technology
25 PUBLICATIONS **372** CITATIONS
SEE PROFILE

Available from: Zifu Li
Retrieved on: 01 February 2016

Langmuir

Article

pubs.acs.org/Langmuir

Stabilization of Colloidal Suspensions: Competing Effects of Nanoparticle Halos and Depletion Mechanism

Xiaochen Xing, Guanqing Sun, Zifu Li, and To Ngai*

Department of Chemistry, The Chinese University of Hong Kong, Shatin, New Territories, Hong Kong

Supporting Information

ABSTRACT: Bimodal colloidal mixtures of nanoparticles and microparticles may show different phase behaviors depending upon the interparticle interaction of both species. In the present work, we examined the stabilization of spherical microparticles using highly charged, spherical nanoparticles. Total internal reflection microscopy (TIRM) was used to measure the interaction forces between a charged microparticle and flat glass substrate in aqueous solutions at varying volume fractions of nanoparticles of the same sign. We found that, in the system containing of highly charged nanoparticles, microparticle, and glass substrate, non-adsorbing charged nanoparticles in solution did not lead to depletion attraction. Instead, the addition of nanoparticles was to consistently create a repulsive force between the microparticle and glass substrate even at a very low nanoparticle volume fraction. This result might attributed to the formation of thin shells (halos) with a high local nanoparticle volume fraction to the region near the glass surface, resulting in electrostatic repulsion between the decorated surfaces. This study demonstrates that nanoparticle halos can also arise in binary systems of mutually but highly repulsive microparticle/nanoparticle dispersions.

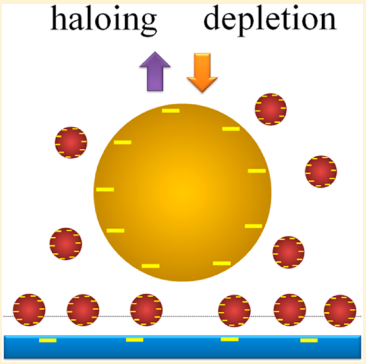

INTRODUCTION

The use of nanometer-sized particles, such as micelles, polymers, polyelectrolytes, and inorganic particles, to manipulate the interaction forces between larger colloidal particles (microparticles) has been investigated for many decades. This is because the applications of colloidal particles in many aspects often involve the use of nanometer-sized polymers or particles (hereafter called nanoparticles). Examples include cosmetics,[1] water treatment,[2] foodstuffs,[3] paints,[4] and inks,[5] only to mention a few. Nanoparticles may be adsorbed to the colloidal particles, chemically attached to their surfaces, or free in solution. Whatever form nanoparticles take, their presence has a major effect on colloidal stabilization.

If the nanoparticles do not adsorb onto the surfaces, a traditional view is that nanoparticles in aqueous solution can promote flocculation of stable colloidal dispersions through an entropic depletion interaction.[6−8] Asakura and Oosawa were the first to describe this force and its origins in the early 1950s.[9] The term "depletion" describes the exclusion of these non-adsorbed nanoparticles from the gap region between large colloidal particles that arise when their separation distance becomes less than the characteristic nanoparticle size. The resulting concentration gradient between the gap region and bulk solution leads to an attractive force, whose magnitude depends upon the nanoparticle concentration, their surface charge, and the size ratio of large to small species. Depletion forces have been extensively studied in the presence of non-adsorbing nanoparticle suspensions,[10] surfactant micellar solution,[11,12] polymer solutions,[13,14] and charged polyelectrolytes.[15,16] Moreover, it is also shown that, as the concentration of nanoparticles increases beyond the dilute limit, the ordering of the nanoparticles under confinement at a higher particle concentration can lead to an oscillatory force profile between the large colloidal particles.[17]

It should be mentioned that the majority of the studies discussed above, especially in systems containing nanoparticles in solutions, have mainly paid attention to systems in which the introduced nanoparticles exhibited little adsorption. Specifically, theoretical studies commonly assume no adsorption, while experimental investigations have attempted to use components where adsorption was negative. Recently, however, researchers have begun to examine systems in which the large colloidal particle−nanoparticle interaction is much weaker or even slightly attractive. A new stabilization mechanism, known as nanoparticle haloing, has been suggested for bimodal colloidal mixtures by adding highly charged nanoparticles to a negligibly charged colloidal suspension.[18] In this case, charged nanoparticles surround neutral microparticles, decreasing van der Waals attractions between the microparticles. Stabilization by nanoparticle haloing has been observed for larger diameter silica particles by small highly charged zirconia[18] and polystyrene (PS),[19] and similar stabilization of single-walled carbon nanotube (SWNT) dispersions has been observed by charged nanoparticles.[20] The key feature of nanoparticle haloing highlights a new pathway of using nanoparticles as a tool to tailor the stability of a dispersion.

Very recently, Ji and Walz[21] have also investigated the potential use of highly charged, spherical nanoparticles to

Received: September 3, 2012
Revised: October 30, 2012
Published: November 1, 2012

 © 2012 American Chemical Society dx.doi.org/10.1021/la303547m | Langmuir 2012, 28, 16022−16028

control the forces between a spherical microparticle and a charged plate. It was found that, except for cases where the nanoparticle−microparticle pair potential was strongly repulsive (highly charged for both the nanoparticle and microparticle), sufficient nanoparticle deposition to the microparticle and flat plate occurred even with the addition of relatively low concentrations (e.g., 0.1 vol %) of the nanoparticles. Such irreversible deposition, as confirmed by their experiments, could obviously lead to an increased repulsion between the microparticle and plate. The mechanism involved would simply be an increase in the effective charge density of both the microparticle and plate because of the deposited charged nanoparticles. More importantly, this increased repulsive force did not disappear upon flushing the nanoparticles out of the system, indicating that the nanoparticles were held in relatively deep energy wells. Their results illustrate the challenges associated with using charged nanoparticles as a tool for manipulating colloidal stability.

Despite the studies referenced above, we herein conduct a comprehensive experimental study in a bidispersed system, in which we directly measure the interaction force between a charged micrometer-sized colloidal particle and flat glass substrate in the presence of charged nanoparticles of the same sign in aqueous solution. Our goal is to understand how nanoparticles alter forces between microparticles as a function of the nature of the microparticle−nanoparticle interaction at different volume fractions. Two different types of experiments were performed. First, direct measurement of the force profiles between a PS microparticle (diameter of ∼6 μm) and a glass substrate in the presence of charged PS nanoparticles (diameter of ∼320 nm) was obtained using the technique of total internal reflection microscopy (TIRM). We intend to understand the initial effect of adding the nanoparticles to the microparticle solution and the characteristic and nature of the forces produced by the nanoparticles. Second, to regulate the charge density of the nanoparticle and, thus, the strength and range of the microparticle−nanoparticle interaction, PS nanoparticles were coated with a soft hydrogel layer and we investigated the effect of such core−shell nanoparticles on the interaction force profile between microparticles. This study allows for precise evaluation of how the nature of the nanoparticle−microparticle interaction alters the microparticle−plate force profile.

EXPERIMENTAL SECTION

Sample Preparation. Micrometer-sized PS sulfonate latex particles with a diameter of ∼6.0 μm (CV 4.1%) were purchased from Interfacial Dynamics Co., Portland, OR, and used without further treatment. Silica microscopy slides (BK-7 glass, Fischer Scientific Co.) were first thoroughly cleaned by ultrasonication for 15 min in ethanol and then dried by blowing with highly pure nitrogen. After that, the dried slides were dipped in 5% HF solution and then washed with deionized water again. The treated slides were kept in ethanol and further cleaned by an ultraviolet (UV)-zone plasma cleaner (Harrick Sci. Co.) before assembling the sample cell. The NaCl (GR from BDH) was heated at ∼200 °C for ∼2 days to remove organic impurities. Water was purified with an inverse osmosis filtration (Nano Pure, Barnstead) until its resistivity reached 18.2 MΩ cm at 20 °C and was then filtered with a Milipore polytetrafluoroethylene (PTFE) 0.45 μm hydrophilic filter.

PS nanoparticles were synthesized using surfactant-free emulsion polymerization. Typically, 5.01 g of styrene, 0.151 g of divinylbenzene (DVB), and 0.251 g of methacrylate acid (MAA) were dissolved in 150 mL of deionized water in a 250 mL two-neck reactor fitted with a nitrogen bubbling inlet and outlet and a reflux condenser and stirred with a stir bar. After the solution was stirred for 40 min at room temperature under nitrogen bubbling, the polymerization was initiated by adding 0.140 g of potassium persulfate (KPS) dissolved in 10 mL of deionized water. The reaction mixture was kept at 70 °C for 24 h; the pH of the dispersion after the reaction was 3.7; and the resultant nanoparticles were centrifuged at 10 000 rpm for 1 h to remove the unreacted reagents or polymer chains. The synthesized carboxylic-acid-coated PS nanoparticles have an average diameter of around 332 nm and are narrowly distributed as determined by dynamic laser light scattering (DLS, ALV5000) (see Figure S1 of the Supporting Information).

Poly(styrene-*co*-*N*-isopropylacrylamide) (PS-*co*-NIPAm) core−shell nanoparticles were synthesized using a one-pot, surfactant-free emulsion polymerization.[22,23] Typically, 1.036 g of NIPAm, 8.47 g of styrene, 0.034 g of *N*,*N*′-methylenebis(acrylamide) (MBAA), and 0.043 g of MAA were dissolved in 140 mL of deionized water in a 250 mL two-neck reactor fitted with a nitrogen bubbling inlet and outlet and a reflux condenser and stirred with a magnetic stir bar. Then, the solution mixture was adjusted to pH 10 with sodium hydroxide solution. After stirring the solution for 40 min at 25 °C under nitrogen bubbling, the polymerization was initiated by adding 0.113 g of KPS dissolved in 10 mL of deionized water. The reaction mixture was kept at 70 °C for 9 h. The resultant particles were cleaned by centrifugation 3 times for approximately 1 h at 10 000 rpm at room temperature to remove any unreacted monomeric or oligomeric species. Then, the nanoparticles were freeze-dried and redispersed with deionized water. The synthesized PS-*co*-NIPAm core−shell particles have an average diameter of about 324 nm, as determined by DLS (see Figure S2 of the Supporting Information), which is almost the same in size as the used PS nanoparticles. Note that the synthesized core−shell particles are composed of a high content of styrene monomers, about 88.4% of the total mass. The inset picture of Figure S2 of the Supporting Information confirms that the prepared particles are spherical and with PS as the core and PNIPAm as the shell. The thickness of the PNIPAm shell is around 40−50 nm. The addition of NIPAm to the synthesis adds soft, hydrogel-like qualities that provide particle flexibility.

Total Internal Reflection of Microscopy (TIRM). The interaction potential profiles between a single PS microparticle and the hydrophilic glass surface in the presence of both PS and PS-*co*-NIPAm nanoparticle solutions were determined by TIRM. Details about TIRM has been described elsewhere.[24] In a TIRM measurement, an evanescent wave, which decays exponentially with the distance from the interface, is generated at the liquid/solid surface by a total internal reflection within the glass slide. Any particle located near the interface will scatter the incident evanescent wave. The scattered intensity depends upon the distance between the sphere particle and the surface of the glass slide as[24]

$$I(h) = I_0 \exp(-\beta h) \tag{1}$$

where h is the distance from the sphere particle to the slide surface, I_0 is the "stuck" particle intensity, when $h = 0$, and β^{-1} is the characteristic penetration length. Measuring the scattered intensity over a sufficiently long period provides a histogram of the separation distance, $p(h)$, which can be related to the total potential energy, $\Phi(h)$, at that point through a Boltzmann relationship[24]

$$p(h) = A \exp\left[-\frac{\Phi(h)}{k_B T}\right] \tag{2}$$

where A is a constant normalizing the integrated distribution to unity. The potential energy profile is obtained by inverting the distribution. Typically, we first measured the potential energy between a PS microparticle and a hydrophilic glass surface in pure NaOH/HCl solution with the certain pH values. After that, nanoparticles dispersed in aqueous solution at corresponding pH were introduced in the sample cell to replace the pure NaOH/HCl solution by a flex tubing pump (Master Flex), while the PS microparticle was trapped in place by optical tweezers. At least ∼20 mL of fluid was used to change solutions (changing the volume inside the sample cell at least 10 times). After complete replacement and waited for 30 min, the

dx.doi.org/10.1021/la303547m | *Langmuir* 2012, 28, 16022−16028

interaction potentials between the PS microparticle and the glass surface in the presence of the nanoparticle solution were measured. In the next step, the particle was trapped again and the sample cell was rinsed with another nanoparticle solution. The interaction between the PS particle and surface was measured after the rinsing. Note that, in this manner, we can exchange the solution inside the sample cell between the pure NaOH/HCl solution and nanoparticle solution repeatedly but keep using the same PS microparticle and glass substrate, which can significantly reduce the effects of particle and surface variations.

The last portion of this experiment is the distance calibration of the height between particle and surface where a high concentration of slat solution (100 mM) was pumped in to screen the repulsion levitating the PS particle. The particle will then "stuck" to the plate, and the scattering intensity was measured. A region where there are no particles in the microscopy field was then selected to determine the background scattering intensity. The difference between the average of the "stuck" particle intensity and the average of the background intensity is then taken to be I_0 in eq 1.

ζ Potentials. The ζ potentials of the micro- and nano-sized particles were measured with a commercial ζ-potential spectrometer (ZetaPlus, Brookhaven) at a pH value of 10.25. Table 1 summarizes

Table 1. Approximate ζ Potentials of the PS Microparticles, PS Nanoparticles, PS-*co*-NIPAm Nanoparticles, and Glass Plate at the Experimental Conditions Used in the Experiments

pH	$\xi_{microparticle}$ (mV)	$\xi_{PS\ nanoparticle}$ (mV)	$\xi_{PS\text{-}co\text{-}NIPAm\ nanoparticle}$ (mV)	ξ_{plate} (mV)
10.25	−90	−60	−20	−80

the ζ potentials of the PS microparticles, PS nanoparticles, PS-*co*-NIPAm nanoparticles, and glass slides at pH 10.25 used in the force experiments. For PS microparticles, the average ζ potential measured in pH 10.25 is approximately −90 mV, indicating that they are highly negatively charged at a high pH value. For synthesized PS nanoparticles, the ζ potential is approximately −60 mV when the pH value is raised to 10.25. This is attributed to the fact that functional MAA groups were co-polymerized onto the particle surface. As the pH value of the solution increases, deprotonation of the carboxylic groups (−COOH) on the surfaces results in the surface charge increasing significantly; therefore, the nanoparticles became highly negatively charged particles. However, the ζ potentials of the core−shell PS-*co*-NIPAm nanoparticles were determined as −20 mV at solution pH 10.25, indicating that coating of the NIPAm hydrogel layer has greatly shielded the electric charge density of the resulting nanoparticles. For glass slides, we took the ζ potential values reported by Ji and Walz;[21] they were approximately −80 mV at pH 10.24.

RESULTS AND DISCUSSION

Force Profiles in the Presence of PS Nanoparticles at pH 10.25. The influence of the PS nanoparticles on the potential energy profiles between the microparticle and glass substrate is shown in Figures 1 and 2. Specifically, Figure 1 shows interaction potentials that were measured at a solution pH value of 10.25, and nanoparticle volume fractions of 0, 2×10^{-4}, 3×10^{-4}, 4×10^{-4}, 5×10^{-4}, 6×10^{-4}, 8×10^{-4}, and 1×10^{-3} were used. It can be clearly seen that, at pH 10.25, the microparticle−plate separation distance, h, increases consistently with an increasing nanoparticle volume fraction, suggesting that there is a repulsive force that also increases consistently when the nanoparticles are introduced. Even at 2×10^{-4}, the separation distance is substantially increased above that with no nanoparticles (around 33.5 nm). The following equation

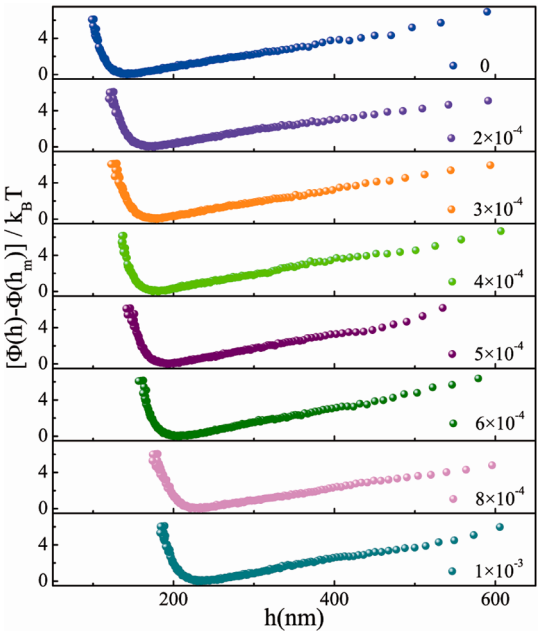

Figure 1. Measured interaction potential profiles between the microparticle and glass substrate at varying nanoparticle volume fractions with solution pH 10.25.

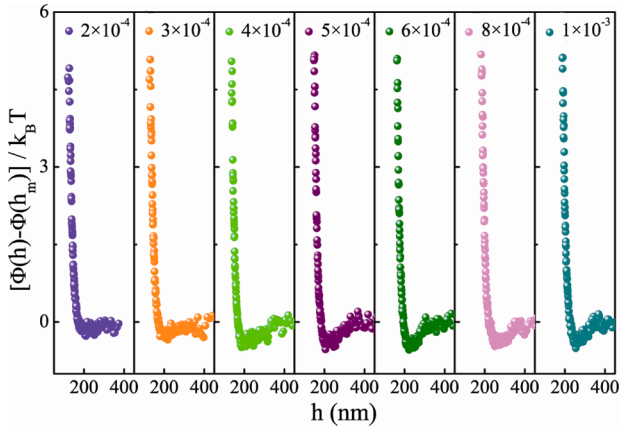

Figure 2. Measured net interaction potential profiles between the microparticle and glass substrate at varying nanoparticle volume fractions with solution pH 10.25. The gravity of all of the interaction potentials has been subtracted.

$$\Phi(h) = B \exp(-\kappa h) + Gh \tag{3}$$

where B is a parameter related to surface potential, κ is the Debye parameter, and G is the net weight of the microparticle, was used to fit the measured interaction potentials at each nanoparticle volume fraction at pH 10.25, and the results were summarized in Table 2. As seen, the measured decay length, λ_D, almost equals the calculated bulk solution decay length ($\kappa^{-1} \approx$ 20 nm), indicating that the observed repulsive force was electrostatic in origin. It is worth pointing out that the same PS microparticle was used in the consecutive potentials before and after introducing nanoparticles. In this way, the contribution of gravity was subtracted from all measured potentials, and the net potential profiles were plotted in Figure 2. As seen, in the presence of highly charged nanoparticles, a slight attractive interaction force ($\sim -1 k_B T$) can be found in the potential profiles with the separation distance up to ~200 nm. The

dx.doi.org/10.1021/la303547m | Langmuir 2012, 28, 16022−16028

Table 2. Fitting Results of the Debye Length of the Measured Potential Files between a PS Sphere and Glass Surface in Each Step and the Equilibrium Distance from the Flat Surface at pH 10.25

c (vol %)	0	0.02	0.04	0.05	0.06	0.08	0.1
λ_D (nm)	11.5	15.3	13.1	13.8	13.5	17.4	12.7
h_m (nm)	142.2	175.7	181.0	192.1	206.0	234.4	230.5

magnitude of this attractive force increases with an increasing nanoparticle volume fraction.

The results from the experiments described above show a consistent and straightforward picture of the effects of charged nanoparticles on the interaction energy profile between the microparticle and plate surface. The addition of nanoparticles leads to a repulsive force, which increases substantially with an increasing nanoparticle volume fraction. At pH 10.25, the microparticles (−90 mV), glass substrate (−80 mV), and nanoparticles (−60 mV) were highly negatively charged. Under this experimental condition, adsorption of the nanoparticles onto the microparticle and glass surface should be highly unlikely because of the strong electrostatic repulsion between the microparticle and plate. Direct evidence of this can be seen in the scanning electron microscopy (SEM) pictures shown in Figure S3 of the Supporting Information; no deposition occurs at a pH value of 10.25. Similar to a number of experimental studies,[8,25−29] we initially expect that the effect of the nanoparticles would create a depletion attractive force between the microparticle and glass plate, pushing the microparticle closer to the surface. This attractive force arises from the exclusion of the nanoparticles from the gap region between the microparticle and plate. Conversely, as seen in Figure 1, the addition of nanoparticles produced a pure repulsive force and the separation distance between the microparticle and plate increased significantly as the nanoparticle volume fraction was increased. Figure 2 shows that the long-range depletion was present at a very low nanoparticle concentration (0.03 vol %). This result likely suggests that there is negative absorption or deposition of the nanoparticles onto the microparticle and plate surfaces. However, clearly, this created depletion presented as these nanoparticle volume fractions is much less pronounced than the generated repulsive force in the addition of highly charged nanoparticles.

In 2001, a new stabilization mechanism, known as "nanoparticle haloing", has been suggested by Tohver et al.[18] to account for binary colloidal mixtures, in which microparticles have a low electric surface charge in solution with nanoparticles that have a surface charge of the same sign but of much greater magnitude. The fundamental basis for a nanoparticle halo is that nanoparticles become trapped in shallow energy wells close to the larger surface. In other words, these nanoparticles are "crowded" next to the microparticles because of strong mutual repulsion between them in bulk solution, which, in turn, serves to mitigate the long-range van der Waals attraction. Theoretical calculation and Monte Carlo simulations[30,31] showed that halos could also arise from weak attractive forces between the microparticle and nanoparticles. Experimentally, the direct measurement of this repulsive force in a nanoparticle haloing system was reported by Hong and Willing.[32] Using colloidal probe atomic force microscopy, they measured the force profile between silica surfaces in solution of zirconia nanoparticles at different concentrations. At 10^{-5}, they observed a slight dip in the force profile, which the authors attributed to nanoparticle haloing. However, this phenomenon was never observed at any other nanoparticle concentration, including 10^{-3}, 10^{-4}, and 10^{-6}. Our study, however, showed that, at pH 10.25, the repulsive force was consistently observed with an increasing nanoparticle volume fraction. Considering the presence of a significant fraction of nanoparticle species in the bulk solution and a strong nanoparticle deposition not being likely (see Figure S3 of the Supporting Information), these nanoparticles might reside to the region near the glass surface because it had a relatively low electric surface charge, which eventually gave rise to the effective repulsive force to push the microparticle away. To provide additional evidence of the crowding nanoparticle near the plate surface, we measured the scattered evanescent wave light intensity of the sample cell as a function of the nanoparticle volume fraction. As seen in Figure 3, the background noise increased with an increasing nanoparticle volume fraction but the contributed sample intensity was greatly enhanced when the nanoparticle volume fraction was increased, indicating that the number density of the nanoparticles near the plate surface is larger than that in bulk solution. Hence, this is the first study to demonstrate that nanoparticle halos can also arise in binary systems of mutually but highly repulsive microparticle/nanoparticle dispersions, as schematically shown in Figure 4. We believe that this finding will stimulate theoreticians to investigate the interparticle interactions in bidispersed particle suspensions.

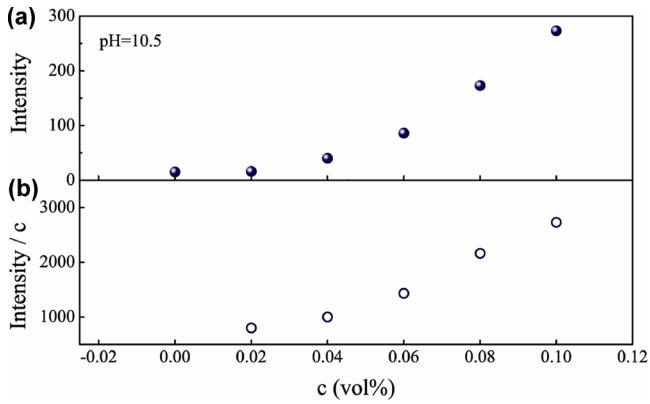

Figure 3. Background intensity versus nanoparticle volume fraction on TIRM: (a) volume fraction dependence of the scattering intensity of nanoparticles and (b) volume fraction dependence of the normalized scattering intensity of nanoparticles.

Direct Measurement of the Interaction Force between Colloidal Particles in a Solution of PS-*co*-NIPAm Nanoparticles. In the studies shown above, one obvious question that arises in interpreting the results is whether the deposition of the nanoparticles should be expected at the experimental conditions. In other words, how the nature of the microparticle (or plate)−nanoparticle interaction should greatly affect the measured microparticle−plate profiles. To gain a deeper insight, we coated the surfaces of highly charged PS nanoparticles with a soft hydrogel layer. In this way, the charge density of the nanoparticles and, thus, the strength and range of the microparticle (plate)−nanoparticle interaction can be

dx.doi.org/10.1021/la303547m | Langmuir 2012, 28, 16022−16028

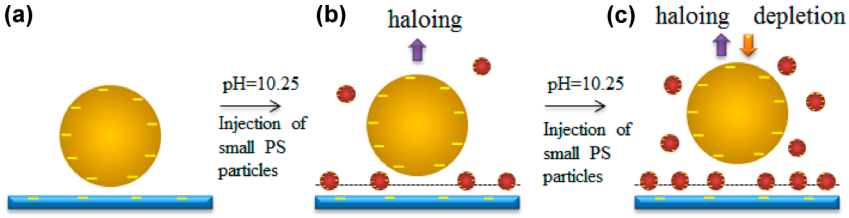

Figure 4. Schematic diagram of the interactions between a probe sphere and a flat surface induced by the PS nanoparticles: (a) initial conditions, (b) nanoparticle halos surrounding the plate to pull the microparticle away, and (c) repulsion induced by nanoparticle halos and depletion attraction existing simultaneously at a higher volume fraction of nanoparticles.

regulated. The following study will investigate how the nature of the nanoparticle−microparticle (plate) interaction alters the microparticle−plate force profile.

Figure 5 shows the interaction potential energy profiles between the PS microparticle and plate surface that were

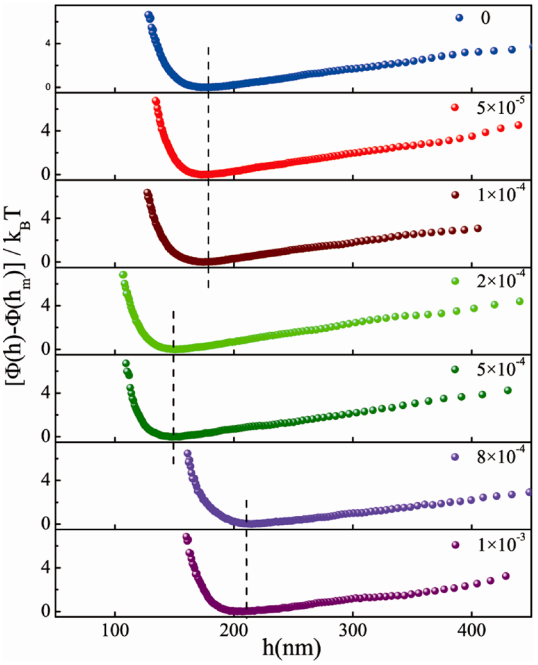

Figure 5. Measured interaction potential profiles between the microparticle and glass substrate at varying PS-*co*-PNIPAm core−shell nanoparticle volume fractions with solution pH 10.25.

measured at a solution pH value of 10.25, and PS-*co*-NIPAm nanoparticle volume fractions of 5×10^{-5}, 1×10^{-4}, 2×10^{-4}, 5×10^{-4}, 8×10^{-4}, and 1×10^{-3} were used. Note that, at pH 10.25, the PS microparticle (−90 mV) and glass substrate (−80 mV) were highly negatively charged, while PS-*co*-NIPAm nanoparticles (−20 mV) were slightly negatively charged. Without the addition of PS-*co*-NIPAm nanoparticles, the interaction potential of the highly negatively charged PS microparticle at height h above the highly negatively glass plate is typically composed of two parts: toward smaller h electrostatic repulsion domains and the major contribution at larger h coming from the gravity. The equilibrium distance, h_m, between the microparticle and plate was about 175 nm.

The effect of adding PS-*co*-NIPAm core−shell nanoparticles to the solution can be summarized as follows: (i) At a low core−shell nanoparticle volume fraction ($<2 \times 10^{-4}$), the addition of core−shell nanoparticles has a much smaller impact on the interaction potential profiles. Actually, the interaction potential measured at 0.01 vol % is almost identical to that with no added core−shell nanoparticles. (ii) At an intermediate core−shell nanoparticle volume fraction ($2 \times 10^{-4} \leq \phi_{nanoparticle} \leq 5 \times 10^{-4}$), separation distance, h, decreased with an increasing nanoparticle volume fraction and the measured interaction potentials were shifted closer to the plate surface, indicating that a long-range attractive force was generated. This can be seen more clearly in the results present in Figure 6, in

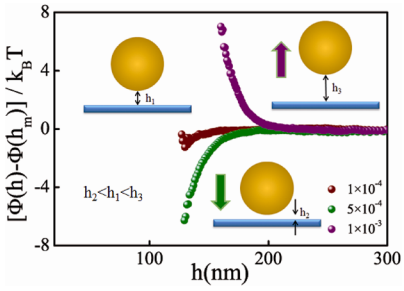

Figure 6. Potential energy subtracted by the potential with no added nanoparticles on TIRM with pH 10.25 as the core−shell nanoparticle volume fraction increases from 2×10^{-4} to 1×10^{-3}.

which the measured potentials were subtracted by the potential with no added nanoparticles. Previous studies have shown that pure PNIPAm chains can be irreversibly absorbed to the glass surface or PS nanoparticles through the hydrophobic interaction or hydrogen bonding.[33] Although different in molecular conformation, the chemical nature of PS-*co*-NIPAm nanoparticles should be the same. In this way, the adsorption of relatively weakly charged, hairy-like core−shell nanoparticles to the microparticle and plate surface can be allowed. Moreover, Ji and Walz also showed that, unless the microparticle−nanoparticle pair potential was strongly repulsive ($>60k_BT$), nanoparticle deposition occurred even at a very low nanoparticle concentration.[21] We infer that the deposition of weakly charged nanoparticles onto the highly charged surfaces reduces the electrostatic interaction between the nanoparticle-decorated microparticle and plate surface, so that the microparticle moves closer to the flat surfaces, which, in turn, eventually facilitates bridging, as schematically shown in Figure 7. (iii) At a high core−shell nanoparticle volume fraction ($\phi_{nanoparticle} \geq 8 \times 10^{-4}$), the separation distance, h, was surprisingly increased, suggesting an enhanced repulsive force in the system (Figure 5). Again, this can be seen more clearly in Figure 6 after the measured potentials were subtracted by the potential with no added nanoparticles. The origin of such repulsion is unclear at this moment. One possible way is that, when more core−shell nanoparticles were added, the surface of both the microparticle and plate may be better covered by the deposited nanoparticles. This soft layer nanoparticle can sustainably generate a steric

dx.doi.org/10.1021/la303547m | *Langmuir* 2012, 28, 16022−16028

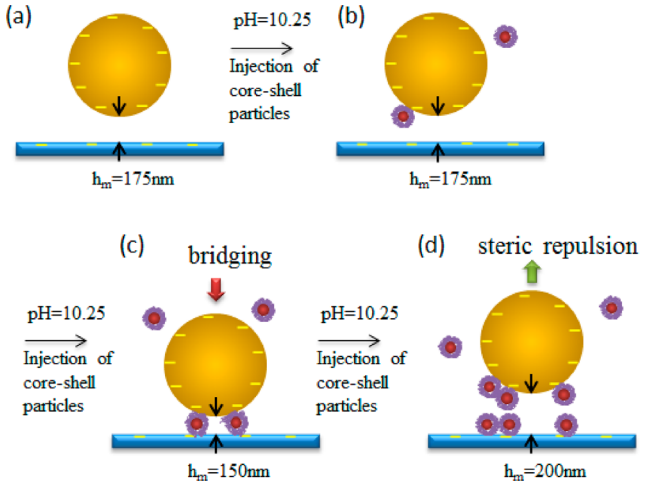

Figure 7. Schematic diagram of the interactions between a probe sphere and a flat surface induced by the PS-*co*-NIPAm core–shell nanoparticles: (a) initial conditions, (b) core–shell particle slightly adsorbing to the microparticle or plate at a low volume fraction of the core–shell particle, (c) attraction by bridging between the microparticle and plate at a medium volume fraction of the core–shell particle, and (d) steric repulsion induced by abundant adsorption between the microparticle and plate at a high volume fraction of the core–shell particle.

repulsive force to overwhelm the attraction, and the microparticle moves far away from the plate surface, as schematically illustrated in Figure 7.

In addition, the effect of adding PS-*co*-NIPAm core–shell nanoparticles to the PS microparticle suspensions was also investigated by optical microscopy at room temperature. Note that, under the optical microscope, only the PS microparticles are visible, while the core–shell nanoparticles are not, because the size is much smaller than the wavelength of visible light. As shown in Figure 8a, PS microparticles were randomly moved in

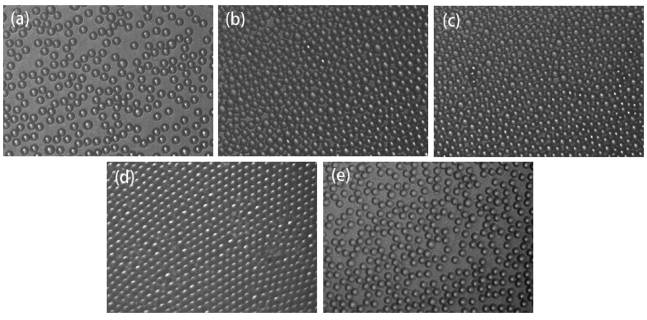

Figure 8. Microscopy photographs of PS microparticles and PS-*co*-NIPAm core–shell nanoparticles mixed suspension. From panels a to e, the core–shell particle concentration is 0.025, 0.05, 0.125, 0.25, and 0.5 vol %, respectively.

the binary suspension with the addition of a small amount of core–shell nanoparticles (0.025 vol %). Interestingly, random closely packed or even crystal-like structures (panels b–d of Figure 8) started to form with the further increasing of the core–shell nanoparticles, indicating that the addition of nanoparticles likely induced an attractive force. This is in good agreement with our TIRM measurements. Dependent upon the adsorption of added nanoparticles or not, this attractive force could arise from either the depletion mechanism or the bridging mechanism. Theoretical calculation by Dickinson pointed out that the addition of a polymer in a small amount (<0.01 vol %) could cause a substantial clustering and gelation of colloidal particles if the polymer can be adsorbed to the colloid particles.[34] Ji and Walz also showed that, unless the microparticle–nanoparticle pair potential was strongly repulsive, nanoparticle deposition occurred even at a very low nanoparticle concentration.[21] Therefore, we would like to attribute the ordered packing of the microparticles to the bridging effect. Again, it was surprising to find that, in the presence of a high nanoparticle concentration (Figure 8e), the binary system transformed from the crystal-like to the random structure. We conjecture that, when there are enough core–shell nanoparticles, the surface of the microparticles could be totally covered by the adsorbed nanoparticles. This soft layer of the nanoparticle might play the role of the stabilizer, and the microparticles are separated again.

CONCLUSION

In summary, we have performed an experimental investigation on the interparticle interaction in the binary particle suspensions. Our results show that the initial addition of charged nanoparticles can alter the interaction force between the charged microparticle and plate surface. For the suspension system where the nanoparticles, microparticle, and plate were highly charged, the adsorption of nanoparticles was hindered because of the strong electrostatic repulsion between the microparticle and plate. Unprecedentedly, the addition of nanoparticles also produced a repulsive force. This observed trend is substantially different from that in systems where the nanoparticle–microparticle/plate was strongly repulsive; the effect of the nanoparticles was to create an attractive depletion force between the microparticle and plate. Our results suggested that these nanoparticles might reside in the region near the glass surface because it had a relatively low electric surface charge, which eventually gave rise the effective repulsive force. This is the first study to demonstrate that nanoparticle halos can also arise in binary systems of mutually but highly repulsive microparticle/nanoparticle dispersions. We believe that this finding will stimulate theoreticians to investigate the nature of such induced interparticle interactions.

Coating the charged nanoparticles with a soft hydrogel layer can regulate the strength and range of the microparticle (plate)–nanoparticle interaction. We showed that charge shielding allowed for the deposition of core–shell nanoparticles onto the highly charged surfaces, which, in turn, reduced the electrostatic interaction between surfaces, eventually leading to bridging. When more core–shell nanoparticles were presented, the surface of both the microparticle and plate might be totally covered by the deposited nanoparticles. This soft layer nanoparticle can sustainably generate a steric repulsive force to overwhelm the attraction. Our results thus highlight the challenges associated with using charged nanoparticles as a tool to regulate stability in the binary particle systems.

ASSOCIATED CONTENT

Supporting Information

Typical hydrodynamic radius distribution of the synthesized PS particles (Figure S1) and synthesized PS-*co*-NIPAm nanoparticles (Figure S2) and SEM micrographs of PS microparticles mixed with nanoparticles (Figure S3). This material is available free of charge via the Internet at http://pubs.acs.org.

dx.doi.org/10.1021/la303547m | *Langmuir* 2012, 28, 16022–16028

AUTHOR INFORMATION

Corresponding Author

*Telephone: (852) 3943-1222. Fax: (852) 2603-5057. E-mail: tongai@cuhk.edu.hk.

Notes

The authors declare no competing financial interest.

ACKNOWLEDGMENTS

The financial support of this work by the Hong Kong Special Administration Region (HKSAR) General Research Fund (CUHK402809, 2160387) is gratefully acknowledged.

REFERENCES

(1) Sonneville-Aubrun, O.; Simonnet, J. T.; L'Alloret, F. Nanoemulsions: A new vehicle for skincare products. *Adv. Colloid Interface Sci.* **2004**, *108−109*, 145.

(2) Hopkins, E. S. Colloidal chemistry in water treatment. *Ind. Eng. Chem.* **1940**, *32*, 263.

(3) Skelhon, T. S.; Grossiord, N.; Morgan, A. R.; Bon, S. A. F. Quiescent water-in-oil pickering emulsions as a route toward healthier fruit juice infused chocolate confectionary. *J. Mater. Chem.* **2012**, *22*, 19289.

(4) Farrokhpay, S.; Morris, G. E.; Fornasiero, D.; Self, P. Titania pigment particles dispersion in water-based paint films. *JCT Res.* **2006**, *3*, 275.

(5) Chrisey, D. B. Materials processing—The power of direct writing. *Science* **2000**, *289*, 879.

(6) Mao, Y.; Cates, M. E.; Lekkerkerker, H. N. W. Depletion force in colloidal systems. *Phys. A* **1995**, *222*, 10.

(7) Drelich, J.; Long, J.; Xu, Z.; Masliyah, J.; Nalaskowski, J.; Beauchamp, R.; Liu, Y. AFM colloidal forces measured between microscopic probes and flat substrates in nanoparticle suspensions. *J. Colloid Interface Sci.* **2006**, *301*, 511.

(8) Piech, M.; Walz, J. Y. The structuring of nonadsorbed nanoparticles and polyelectrolyte chains in the gap between a colloidal particle and plate. *J. Phys. Chem. B* **2004**, *108*, 9177.

(9) Oosawa, F.; Asakura, S. Surface tension of high-polymer solutions. *J. Chem. Phys.* **1954**, *22*, 1255.

(10) Sharma, A.; Walz, J. Y. Direct measurement of the depletion interaction in a charged colloidal dispersion. *J. Chem. Soc., Faraday Trans.* **1996**, *92*, 4997.

(11) Richetti, P.; Kekicheff, P. Direct measurement of depletion and structural forces in a micellar system. *Phys. Rev. Lett.* **1992**, *68*, 1951.

(12) Ducker, W. A.; Senden, T. J.; Pashley, R. M. Direct measurement of colloidal forces using an atomic force microscope. *Nature* **1991**, *353*, 239.

(13) Milling, A. J.; Kendall, K. Depletion, adsorption, and structuring of sodium poly(acrylate) at the water−silica interface. 1. An atomic force microscopy force study. *Langmuir* **2000**, *16*, 5106.

(14) Bowden, N.; Terfort, A.; Carbeck, J.; Whitesides, G. M. Self-assembly of mesoscale objects into ordered two-dimensional arrays. *Science* **1997**, *276*, 233.

(15) Horozov, T. S.; Binks, B. P. Particle behaviour at horizontal and vertical fluid interfaces. *Colloid Surf., A* **2005**, *267*, 64.

(16) Park, B. J.; Furst, E. M. Fabrication of unusual asymmetric colloids at an oil−water interface. *Langmuir* **2010**, *26*, 10406.

(17) Crocker, J. C.; Matteo, J. A.; Dinsmore, A. D.; Yodh, A. G. Entropic attraction and repulsion in binary colloids probed with a line optical tweezer. *Phys. Rev. Lett.* **1999**, *82*, 4352.

(18) Tohver, V.; Smay, J. E.; Braem, A.; Braun, P. V.; Lewis, J. A. Nanoparticle halos: A new colloid stabilization mechanism. *Proc. Natl. Acad. Sci. U.S.A.* **2001**, *98*, 8950.

(19) Chan, A. T.; Lewis, J. A. Electrostatically tuned interactions in silica microsphere−polystyrene nanoparticle mixtures. *Langmuir* **2005**, *21*, 8576.

(20) Zhu, J.; Yudasaka, M.; Zhang, M.; Iijima, S. Dispersing carbon nanotubes in water: A noncovalent and nonorganic way. *J. Phys. Chem. B* **2004**, *108*, 11317.

(21) Ji, S. X.; Herman, D.; Walz, J. Y. Manipulating microparticle interactions using highly charged nanoparticles. *Colloid Surf., A* **2012**, *396*, 51.

(22) Hellweg, T.; Dewhurst, C. D.; Eimer, W.; Kratz, K. PNIPAm-*co*-polystyrene core−shell microgels: Structure, swelling behavior, and crystallization. *Langmuir* **2004**, *20*, 4330.

(23) McGrath, J. G.; Bock, R. D.; Cathcart, J. M.; Lyon, L. A. Self-assembly of "paint-on" colloidal crystals using poly(styrene-*co*-*N*-isopropylacrylamide) spheres. *Chem. Mater.* **2007**, *19*, 1584.

(24) Prieve, D. C. Measurement of colloidal forces with TIRM. *Adv. Colloid Interface Sci.* **1999**, *82*, 93.

(25) Weronski, P.; Walz, J. Y. An approximate method for calculating depletion and structural interactions between colloidal particles. *J. Colloid Interface Sci.* **2003**, *263*, 327.

(26) Tulpar, A.; Van Tassel, P. R.; Walz, J. Y. Structuring of macroions confined between like-charged surfaces. *Langmuir* **2006**, *22*, 2876.

(27) Fazelabdolabadi, B.; Walz, J. Y.; Van Tassel, P. R. Influence of charged nanoparticles on colloidal forces: A molecular simulation study. *J. Phys. Chem. B* **2009**, *113*, 13860.

(28) Jin, F.; Gong, X. J.; Ye, J.; Ngai, T. Direct measurement of the nanobubble-induced weak depletion attraction between a spherical particle and a flat surface in an aqueous solution. *Soft Matter* **2008**, *4*, 968.

(29) Xing, X. C.; Li, Z. F.; Ngai, T. pH-controllable depletion attraction induced by microgel particles. *Macromolecules* **2009**, *42*, 7271.

(30) Liu, J.; Luijten, E. Colloidal stabilization via nanoparticle halo formation. *Phys. Rev. E: Stat., Nonlinear, Soft Matter Phys.* **2005**, *72*, No. 061401.

(31) Liu, J. W.; Luijten, E. Stabilization of colloidal suspensions by means of highly charged nanoparticles. *Phys. Rev. Lett.* **2004**, *93*, 247802.

(32) Hong, X. T.; Willing, G. A. Transition force measurement between two negligibly charged surfaces: A new perspective on nanoparticle halos. *Langmuir* **2009**, *25*, 4929.

(33) Gong, X. J.; Xing, X. C.; Wei, X. L.; Ngai, T. Direct measurement of weak depletion force between two surfaces. *Chin. J. Polym. Sci.* **2011**, *29*, 1.

(34) Dickinson, E. On flocculation and gelation in concentrated particulate systems containing added polymer. *J. Chem. Soc., Faraday Trans.* **1995**, *91*, 4413.